CHARACTERIZATION OF MICROWAVE GAUSSIAN PULSE LIGHT TRANSMISSION IN PLASMA

Muyessar·MAMATZUNUN[1], Patiman·A[1], Yanxiang SHI[2], Yantong WANG[1,2*]

This paper presents an investigation into the transmission characteristics of Microwave Gaussian pulse light in plasma, employing the WKB method and the Comsol Multiphysics software. This study examines the propagation characteristics of Microwave Gaussian pulse light with varying frequencies, wave modes, and mode numbers in a plasma medium. A theoretical analysis and numerical simulation are employed to investigate these characteristics. This study examines the impact of Microwave Gaussian pulse light on the electron rate distribution, collision power loss, and plasma power deposition when traversing a plasma medium. It was demonstrated that the frequency of the Microwave Gaussian pulse light has a negligible impact on the electron rate distribution within the plasma. Nevertheless, it exerts a more pronounced influence on the electron rate distribution and collision power loss generated by ionization, with the electron rate and collision power loss being larger in the TM mode. The findings indicate that the impact of waves with higher mode numbers on plasma ionisation is more significant than that of TM waves with lower mode numbers. Moreover, the transmission of a TM wave with an identical number of modes and a TEM wave illustrates that different wave modes can influence plasma ionization. Moreover, the effect of plasma turbulence on the propagation of Microwave Gaussian pulse light is investigated. The findings suggest that turbulence-induced energy transfer results in an increase in the electron rate and power loss, as well as a change in the distribution of power deposition. The findings of this study provide a basis for further investigation into the propagation characteristics of Microwave Gaussian pulse light in plasma, which is of paramount importance for the advancement of laser applications in plasma media.

Keywords: Plasma, Gaussian pulse, Plasma turbulence, WKB method, Numerical simulation.

1.Introduction

Laser-plasma interaction is an important research area for scientists in the field of plasma physics, optics and communications. Plasma is a fourth state material composed of free electrons and ions, which widely exists in nature, such as the solar wind, the Earth's ionosphere, etc., and with the emergence of a variety of artificial plasma, plasma technology has a wide range of applications in many

[1] College of Electronics Engineering, Yili Normal University, Yining, China
[2] Laboratory of Signal Detection and Control Technology, Yining, China, email: wyt6319@163.com

fields, such as nuclear fusion, materials processing and communications. Over the past two decades, researchers have conducted extensive research on a range of topics related to Laser-driven Accelerators [1-3], Ionospheric Radio Wave Propagation [4-7], Resonance Absoption [8-11], and hypersonic vehicle-ground communication [12]. These studies all deal with the fundamental problem of laser propagation in plasma. Microwave Gaussian pulse light exhibits favorable focusing and propagation characteristics, and its light intensity distribution adheres to a Gaussian function law. This is a prevalent type of optical signal in optics and communication technology, occupying a pivotal role in laser technology, power deposition, and ultra-wideband optical communication. The study of Microwave Gaussian pulse light transmission in plasma not only contributes to a deeper understanding of the basic laws governing the interaction between plasma and optical signals, but also has significant practical and research implications in the field of communication.

The propagation of Gaussian pulses in plasma has been extensively studied both at home and abroad. Monot et al. first observed the self-channeling properties of intense laser pulses in low-density plasma using Thomson scattering [13]. Chen et al. used a probe spectrometer to record the radial and axial distributions of the laser pulse and the plasma electron density distribution at different moments of the laser pulse transmission in a jet plasma [14]. He et al. investigated the coherent control of plasma dynamics in laser wake field electron acceleration experiments [15]. Khn et al. modeled the effect of plasma turbulence on microwave transport using the FDTD method [16]. Li et al. obtained anisotropic spatial distribution data of refractive index fluctuations in hypersonic turbulence from experimental images of hypersonic turbulence, and modeled the anisotropic power spectrum of hypersonic plasma turbulence [17]. Malik et al. generated terahertz radiation in a density-modulated "cold" magnetized plasma by mixing with a Hermite-Cosh-Gaussian (HChG) Gaussian laser beam [18]. Iantchenko et al. conducted experimental and computational studies on plasma turbulence in tokamak fusion plasma [19]. Mane et al. investigated the propagation characteristics of a Gaussian laser beam in a collisionless magnetized plasma [20]. Existing studies provide valuable theoretical models and experimental data for the study of Microwave Gaussian pulse light-plasma interaction, but there is a lack of studies on the interaction of Microwave Gaussian pulse light sources of different modes and modes with plasmas of different medium models.

In this paper, the propagation characteristics of Microwave Gaussian pulse light in a uniform and a plasma considering the turbulence effect are investigated by numerical simulation using Comsol Multiphysics software based on the improved WKB method. By constructing Gaussian pulses with different frequencies, moduli and modes, the effects of Microwave Gaussian pulse light propagating in a uniform plasma medium under the above conditions on the electron velocity dis-

tribution of the plasma, the power loss of the signal and the power deposition are discussed in detail. In addition, the parameters of electron rate distribution, collisional power loss and power deposition of Microwave Gaussian pulse light after passing through a uniform plasma and after taking into account the turbulence effect are compared and analyzed due to the anomalous transfer of transmitted energy due to fluid instability and nonlinear effects in the plasma. This not only lays a foundation for understanding the interaction between Microwave Gaussian pulse light and plasma, but also provides an important basis for studying practical application scenarios such as plasma surface treatment, power deposition, power loss and communication system design.

2. Model Description

2.1 Theoretical Models

2.1.1 Plasma Equations

Solve the wave Eq. (1) based on the high frequency component of the electric field in the frequency domain:

$$\nabla \times \mu_0^{-1} \left(\nabla \times \mathbf{E} \right) - k_0^2 \left(\varepsilon_r - \frac{j\sigma}{\omega \varepsilon_0} \right) \cdot \mathbf{E} = 0 \tag{1}$$

where σ is the conductivity of the plasma and its reciprocal is defined as follows:

$$q n_e \sigma^{-1} = \begin{bmatrix} 1 & -\alpha B_z & \alpha B_y \\ \alpha B_z & 1 & -\alpha B_x \\ -\alpha B_y & \alpha B_x & 1 \end{bmatrix} \tag{2}$$

In Eq. (2), n_e is the electron number density, B is the magnetic field, q represents the electron charge; $\alpha = \dfrac{q}{m_e \left(v_e + j\omega \right)}$, m_e is the electron mass, v_e is the electron-neutral particle collision frequency, ω is the angular frequency. The electron number density and electron energy density can be obtained by solving the following drift and diffusion equations:

$$\frac{\partial}{\partial t} n_e + \nabla \cdot \left[-n_e \left(\mu_e \cdot \mathbf{E} \right) - \mathbf{D}_e \cdot \nabla n_e \right] = R_e \tag{3}$$

$$\frac{\partial}{\partial t} n_\varepsilon + \nabla \cdot \left[-n_\varepsilon \left(\mu_\varepsilon \cdot \mathbf{E} \right) - \mathbf{D}_\varepsilon \cdot \nabla n_\varepsilon \right] + \mathbf{E} \cdot \Gamma_e = R_\varepsilon \tag{4}$$

where R_e characterizes the electron source, R_ε characterizes the energy loss due to inelastic collisions, $\dot{D}_e$ is the electron diffusion coefficient, $\dot{D}_\varepsilon$ is the energy diffusion coefficient, μ_ε is the energy mobility for, and the inverse of the electron mobility can be simplified as:

$$\mu_e^{-1} = \begin{bmatrix} \dfrac{1}{\mu_{dc}} & -B_z & B_y \\ B_z & \dfrac{1}{\mu_{dc}} & -B_x \\ -B_y & B_x & \dfrac{1}{\mu_{dc}} \end{bmatrix} \tag{5}$$

where μ_{dc} is the electron mobility in the absence of a magnetic field. The source coefficients in the above equations are determined by the plasma chemical reaction system and are expressed as rate coefficients. Assume that there are M reactions that produce or consume electrons and P inelastic electron-neutral particle collisions. In general, P >> M. The electron source term is given by the following equation:

$$R_e = \sum_{j=1}^{M} x_j k_j N_n n_e \tag{6}$$

where x_j is the mole fraction of the target substance of the reaction, N_n is the density of the neutral molecule, the electron rate coefficient k_j of reaction *j* can be calculated based on cross-section data:

$$k_j = \gamma \int_0^\infty \varepsilon \sigma_k(\varepsilon) f(\varepsilon) d\varepsilon \tag{7}$$

where, $\gamma = \left(2q/m_e\right)^{1/2}$, ε are energies, $\sigma_k(\varepsilon)$ characterizes the collision cross section, and $f\left(\varepsilon\right)$ is the electron energy distribution function.

The electron energy loss is derived by summing the collision energy losses for all reactions:

$$R_\varepsilon = \sum_{j=1}^{P} x_j k_j N_n n_e \Delta\varepsilon_j \tag{8}$$

where $\Delta\varepsilon_j$ is the energy loss for the reaction *j* and the electron source and inelastic energy losses are calculated automatically by the multiphysics field interface.

The rate distribution function was chosen to be a Maxwell distribution:

$$f(\varepsilon)=\phi^{-\frac{3}{2}}\beta_1\exp\left[-\left(\frac{\varepsilon\beta_2}{\phi}\right)\right] \tag{9}$$

where $\beta_1=\Gamma(5/2)^{3/2}\Gamma(3/2)^{-5/2}$, $\beta_1=\Gamma(5/2)\Gamma(3/2)^{-1}$,Γ is the gamma function and the average electron energy $\phi=n_\varepsilon/n_e$.

2.1.2 Propagation Characteristics of Electromagnetic Waves In The Plasma Layer

When the electromagnetic wave is incident at an angle θ_i to the boundary of the plasma layer, and propagates from the boundary surface $z=0$ to the $z=d$,there are two types of waves propagating forward ($+z$) and backward ($-z$) when propagating in the plasma layer. For TE waves ($E_z=0, H_z\neq 0$,as H waves), the electromagnetic field can be represented as $E_y=E_y^+ + E_y^-$, $H_x=H_x^+ + H_x^-$ .According to the Maxwell's equations[21]:

$$\frac{dE_y^+}{dz}+j\frac{\omega}{c}qE_y^+ +\frac{q'}{2q}E_y^+ =\frac{q'}{2q}E_y^- \tag{10}$$

$$\frac{dE_y^-}{dz}-j\frac{\omega}{c}qE_y^- +\frac{q'}{2q}E_y^- =\frac{q'}{2q}E_y^+ \tag{11}$$

Here, $q^2(z)=n^2(z)-\sin^2\theta_i$, $n(z)$ is the refractive index of the plasma, $n^2(z)=\varepsilon_r(z)$, ε_r is the relative permittivity, and c is the speed of light in vacuum. If the coupling effect is neglected, then the terms on the right side of Eqs. (10) and (11) are zero, and the solution of the equations is the traditional WKB solution The effective conditions for the solution are:

$$\left(\frac{c}{\omega}\right)^2\left|\frac{3}{4}\left(\frac{1}{q^2}\frac{dq}{dz}\right)^2-\frac{1}{2}\left(\frac{1}{q^3}\frac{d^2q}{dz^2}\right)\right|\square\ 1 \tag{12}$$

If we consider the amplitude constant term in the WKB [22] solution as a function of r , then

$E_y^+=A(z)q^{-\frac{1}{2}}\exp\left[-j\frac{\omega}{c}\int_0^z qdz\right]$, $E_y^-=B(z)q^{-\frac{1}{2}}\exp\left[+j\frac{\omega}{c}\int_0^z qdz\right]$, $A(z)$ and $B(z)$ represent the amplitude change terms with respect to the propagation distance r .By substituting E_y^+ and E_y^- into Eqs. (10) and (11), have:

$$\frac{dA(z)}{dz}=\frac{q'}{2q}\exp\left[+j2\frac{\omega}{c}\int_0^z qdz\right]B(z) \tag{13}$$

$$\frac{dB(z)}{dr}=\frac{q'}{2q}\exp\left[-j2\frac{\omega}{c}\int_0^z qdz\right]A(z) \tag{14}$$

When TE waves propagate from the boundary, Eqs. (13) and (14) can be expressed in matrix form:

$$\frac{d}{dz}\begin{bmatrix}A(z)\\B(z)\end{bmatrix}=U_{TE}(z)\begin{bmatrix}A(z)\\B(z)\end{bmatrix} \tag{15}$$

Eq. (15) is the second-order WKB solution that considers coupling effects, $U_{TE}(z)=\frac{q'}{2q}\begin{bmatrix}0 & \exp(+j\varphi)\\ \exp(-j\varphi) & 0\end{bmatrix}$, $\varphi=\frac{2\omega}{c}\int_0^z qdz$. Solving Eq. (15) using the difference transfer matrix method results in:

$$\begin{bmatrix}A(z)\\B(z)\end{bmatrix}=\mathsf{r}\,Q_{0\to z}\begin{bmatrix}A(0)\\B(0)\end{bmatrix} \tag{16}$$

Where, $\dot{Q}_{0\to z}$ represents the transfer matrix of the electromagnetic wave from $z=0$ to $z=d$, $m_{12}(z)=\int_0^z\frac{q'}{2q}\exp(+j\varphi)d\xi$, $m_{21}(z)=\int_0^z\frac{q'}{2q}\exp(-j\varphi)d\xi$, According to Eqs.(15) and (16), the transfer function of the TE wave is given by:

$$H(\omega,d)=\exp(-j\varphi)\sqrt{\frac{q(0)}{q(d)}}\frac{1}{\cosh\left[\sqrt{m_{12}(d)m_{21}(d)}\right]} \tag{17}$$

When the incident wave is a TM wave ($H_z=0, E_z\neq 0$, E wave), the transfer function is written as:

$$H(\omega,d)=\exp(-j\varphi)\sqrt{\frac{q(0)\varepsilon_r(d)}{q(d)\varepsilon_r(0)}}\frac{1}{\cosh\left[\sqrt{m_{12}(d)m_{21}(d)}\right]} \tag{18}$$

In this case, $m_{12}(z)=\int_0^z\left(\frac{q'}{2q}-\frac{\varepsilon_r'}{2\varepsilon_r}\right)\exp(+j\varphi)d\xi$,

$m_{21}(z)=\int_0^z\left(\frac{q'}{2q}-\frac{\varepsilon_r'}{2\varepsilon_r}\right)\frac{q'}{2q}\exp(-j\varphi)d\xi$, the effective condition for formula (18) is:

$$\left(\frac{c}{\omega}\right)^2\left|\frac{3}{4}\left(\frac{1}{q^2}\frac{dq}{dz}\right)^2-\frac{1}{2}\left(\frac{1}{q^3}\frac{d^2q}{dz^2}\right)\right|+\frac{1}{q^2}\left[\frac{1}{n}\frac{d^2n}{dz^2}-\frac{1}{2}\left(\frac{1}{n}\frac{dn}{dz}\right)^2\right]\square\ 1 \quad (19)$$

2.2 Simulation model

Assuming there are no coupling effects during the propagation of electromagnetic waves in the plasma layer, and there are no reflected waves in the direction of propagation, we establish a simulation model as shown in Fig.1. The Gaussian pulse light signal is incident obliquely from the boundary plane ($z=0$) to the plasma at an angle of incidence θ_i (in this paper, we consider $\theta_i=0°$ incidence). The plasma sheet is placed at the center of the simulation domain, with both ends truncated by Coordinate-Stretched Perfectly Matched Layers (CPML) to simulate the wave propagation characteristics. The central region in the ensuing simulation result images represents the plasma, while the surrounding area characterizes an infinite domain. Only the plasma region will produce simulation results to depict the interaction between Gaussian pulse light and the plasma.

Fig. 1. Schematic of wave propagation in a plasma plate

This simulation model analyzes the argon plasma chemical reaction system, including elastic collision, excitation collision, direct ionization collision and stepwise ionization collision, and also includes Penning ionization and sub-stable quenching. The specific forms are shown in Table 1.

Comsol Multiphysics realizes the objective of constructing various simulation conditions into partial differential equations based on the finite element analysis method. The goal is to solve specific issues related to the problem under consideration, aiming to achieve simulations that are realistic and comprehensive. The modeling mainly involves importing/building composite bodies, defining qualitatively related materials, flexibly setting simulation fields, solving finite element equations, and post-processing images.

Table 1.

Plasma chemical processes and energy loss

No.	Reaction	Type	$\Delta\varepsilon\left(eV\right)$
R1	$e+Ar=>e+Ar$	Elastic	0
R2	$e+Ar=>e+Ars$	Excitation	11.5
R3	$e+Ars=>e+Ar$	Deexcitation	-11.5
R4	$e+Ar=>2e+Ar+$	Direct Ionization	15.8
R5	$e+Ars=>2e+Ar+$	Stepwise Ionization	4.24
R6	$Ars+Ars=>e+Ar+Ar+$	Penning Ionization	-
R7	$Ars+Ar=>Ar+Ar$	Metastable Quenching	-

This simulation employs Comsol Multiphysics according to the aforementioned principles through the following steps.

1.Add relevant physical domains. The simulation uses the "plasma module" and the "electromagnetic wave frequency domain module" to construct the plasma conductive coupling field through the above multi-physical domain coupling.

$$\sigma_{plasma}=\frac{q^2 n_e}{m_e\left(v_e+j\omega\right)}f\left(\mathsf{r}_B\right) \tag{20}$$

2.Draw the target. Draw the basic model of the simulation according to the principle of Fig.1The plasma size is 0.04m ×0.07m，CPML boundary area size 0.05m ×0.07m;

3.Import boundary conditions and related parameters. This includes the introduction of boundary conditions： The electrical boundary conditions are $-\mathbf{n}\cdot\mathbf{D}=\mathbf{0}$, The flux boundary conditions are $-\mathbf{n}\cdot\Gamma_e=0$、$-\mathbf{n}\cdot\Gamma_\varepsilon=0$， and wall boundary conditions, i.e., the initial conditions for the spatio-temporal evolution equations for the electron and energy densities are：

$$\mathbf{n}\cdot\Gamma_e=\frac{1-r_e}{1+r_e}\left(\frac{1}{2}v_{e,th}n_e\right)-\left(\sum\gamma_j\left(\Gamma_j\cdot\mathbf{n}\right)+\Gamma_t\cdot\mathbf{n}\right) \tag{21}$$

$$\mathbf{n}\cdot\Gamma_\varepsilon=\frac{1-r_e}{1+r_e}\left(\frac{5}{6}v_{e,th}n_\varepsilon\right)-\left(\sum\gamma_j\varepsilon_j\left(\Gamma_j\cdot\mathbf{n}\right)+\varepsilon\left(\Gamma_t\cdot\mathbf{n}\right)\right) \tag{22}$$

The pulse width of the light source is 0.004s, incident from z=0.05m、x=0.035m, the electric field propagation equation satisfies：

$$E\left(z,t\right)=E_0e^{i\left(\beta z-\omega t+\theta\right)} \tag{23}$$

Geometric operations and environmental properties used to satisfy convergence and reduce errors in the finite element solution. The target light source is

introduced by setting the port, and the offset of the port affects the distance between the light source and the plasma in Fig.1;

4.Import formulas and other necessary geometric operations. The input theoretical model corresponds to the corresponding formulas. Other operations refer to data sequence operations, including spatial projection, matrix inversion, reference coordinate system(Cartesian coordinate), etc;

5.Add materials. Set up Isolitron, Infinite Elements, and Light Source, with the Infinite Space material being Air;

6.Meshing and Finite Element Solving. It is able to solve complex discretized problems of anatomical wholes using the transient solver MUMPS, which guarantees problem convergence;

7.Add studies and mapping. The frequency-domain-transient study and the time-period study are used to realize the solution and plotting of parameters such as electron rate distribution, collision power loss, power deposition, and total power density distribution of plasma irradiated by different light sources. The time-scan step is 10^{-4} s. The time-period study is performed in a time-dependent manner.

3. Results And Discussion

3.1 Different Frequency Gaussian Pulse Lasers

The transmission of Microwave Gaussian pulse light of different frequencies in a plasma is discussed using frequency-domain-transient studies. Fig. 2 shows the electron rate transient distributions of two Microwave Gaussian pulse light with spot radius of 1.5 cm, the total power absorbed by the plasma setpoint is 30 W, and frequencies of 2.45 GHz and 24.5 GHz produced by ionization when passing through the plasma for 0.001s.

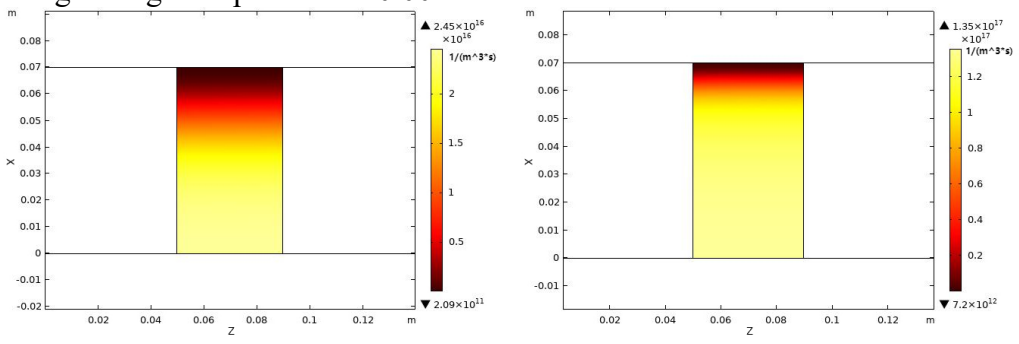

(a) 2.45 GHz (b) 24.5 GHz

Fig. 2. Electron rate distributions of Gaussian pulses of different frequencies passing through the plasma

The simulation results show that the frequency of Microwave Gaussian pulse light does not affect the electron rate distribution inside the plasma, but it can be seen by Eq. (7) that the incident light frequency affects k_j by affecting ε. Using the plas.ne function to solve for the electron density, the maximum value of the electron density in Fig. 2(a) is 7.54×10^{16} m^{-3} and the minimum value is 1.03×10^{11} m^{-3}. The maximum and minimum values of the electron density in Fig.2(b) are 9.79×10^{16} m^{-3} and 3.59×10^{12} m^{-3}, respectively. It can be seen that the frequency of the Microwave Gaussian pulse light has a certain effect on the magnitude of the electron rate generated by the ionization of the plasma. The electron rate increases gradually from the top to the bottom of the plasma, but it does not affect the electron rate distribution in the cross section.

For the location of the electron density maximum, the time-period was used to study the electron density with time for the condition of Fig. 2(a), and the results are shown in Fig.3 The electron density at this location in 0-0.004s with the increase of time firstly rises to the large maximum value, then falls to the minimum value, and finally rises again, and the electron density in this range is of the order of magnitude of 10^{16} , and the difference is only reflected in more than 8 decimal places.

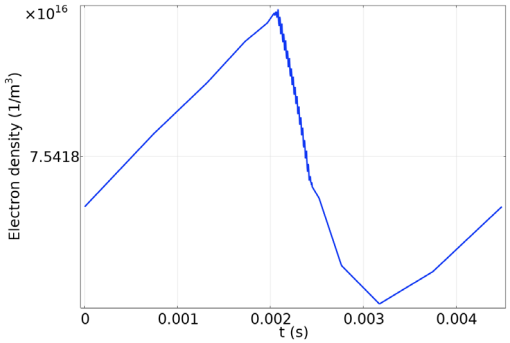

Fig. 3. Variation of electron density with time at the position of maximum electron density

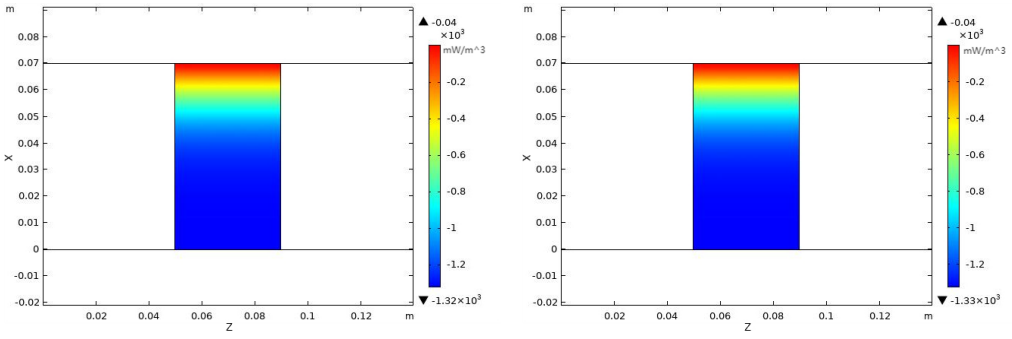

(a) 2.45 GHz (b) 24.5 GHz

Fig. 4. Collisional power loss of Microwave Gaussian pulse light passing through plasma with different frequencies

According to Eq. (7), the distribution of collision power loss generated by Microwave Gaussian pulse light passing through the plasma is consistent with the electron rate distribution of the cross-section, i.e., there is a direct correspondence between the electron rate distribution and the contour of the collision power (energy) loss distribution. Fig.4 shows the collision power loss distribution of Microwave Gaussian pulse light with frequencies of 2.45 GHz and 24.5 GHz through the plasma, and the amplitude of the collision power loss gradually increases from the top to the bottom of the plasma. However, by comparing Fig. 4(a) and Fig. 4(b), it can be seen that the collision power loss at 24.5 GHz frequency is slightly larger than the collision power loss of the pulsed light at frequency 2.45 GHz. This is due to the fact that the increase in frequency leads to a gradual increase in the transmission coefficient and a gradual decrease in the absorption coefficient, which corresponds to a larger k_j value.

3.2 Microwave Gaussian Pulse Light with Different Modes and Mode number

3.2.1 Different mode number

The study of the transmission of Microwave Gaussian pulse light of different mode number in the plasma is realized by using Eq. (18) as the transfer function of the TM wave incident on the plasma. The frequency of the pulsed light is taken to be 2.45 GHz. Fig. 5 shows the electron rate distributions of TM waves of mode number 2 (TM_2 modes or TM_2 waves)and 5(TM_5 modes or TM_5 waves) as they pass through the plasma for 0.001s.

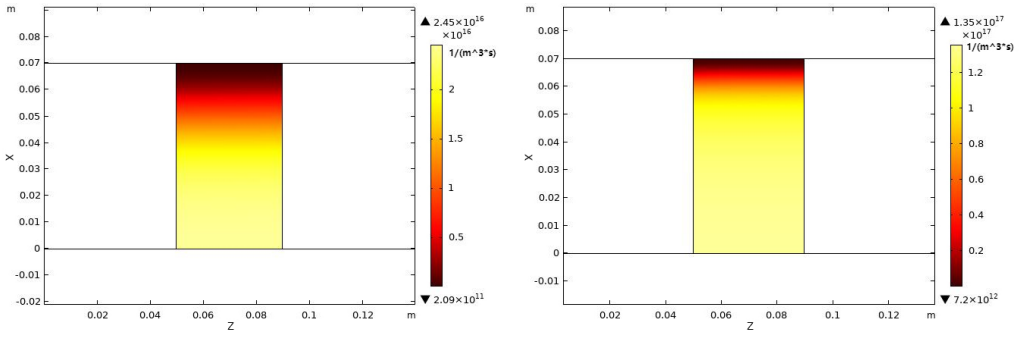

(a) The mode number is 2 (b) The mode number is 5

Fig. 5. Electron rate distribution of TM waves with different mode number produced by plasma ionization

The collision power loss of TM waves with different modes passing through the plasma is investigated, as shown in Fig. 6.

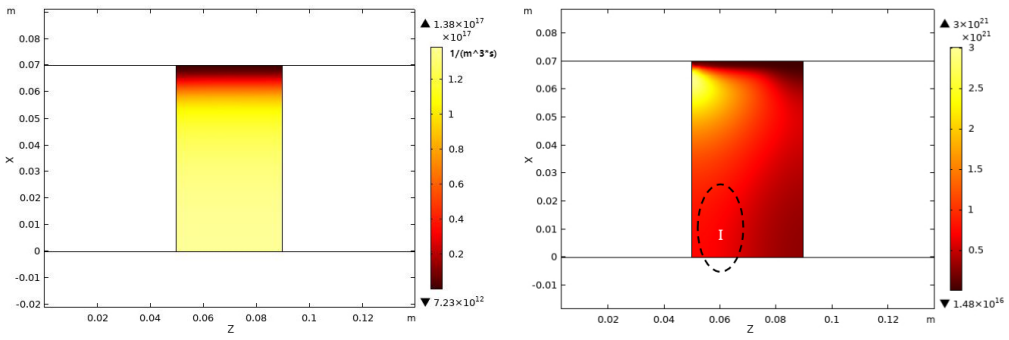

(a) The mode number is 2 (b) The mode number is 5

Fig. 6. Collisional power loss of TM waves of different mode number passing through the plasma

From Fig. 5(a), it can be seen that for low mode number TM waves, the electron rate distribution in the cross section also increases gradually from the top to the bottom of the plasma. However, for high-mode number TM waves, the electron rate distribution of ionization is no longer a gradient distribution with the position of the irradiated side of the plasma, but is "deformed" due to the change of the propagation characteristics caused by the difference of the mode number, as shown in Fig. 5(b). Comparing Figs. 5(a) and 5(b), it can be seen that the higher the mode number, the higher the corresponding electron rate. The maximum value of the electron density in Fig. 5(a) is 9.45×10^{16} m^{-3}, and the minimum value is 1.71×10^{11} m^{-3}. The maximum value of the electron density in Fig. 5(b) is 8.70×10^{20} m^{-3}, and the minimum value is 2.80×10^{15} m^{-3}.

It is not difficult to find that there is still a correspondence between the collision power loss (Fig. 6(a)) and the electron rate distribution (Fig. 5(a)) of the TM waves passing through the plasma with low mode number. However, through Figs. 6(b) and 5(b), it is found that the contours of the collision power loss distribution and the electron rate distribution of the TM wave with high mode number no longer have a direct correspondence in region I. This is due to the fact that the mode number change not only changes the boundary conditions for the solution of the finite element equations by affecting the transfer function, but also the high mode number increases the energy loss, which also leads to the exponential increase of the collision power loss.

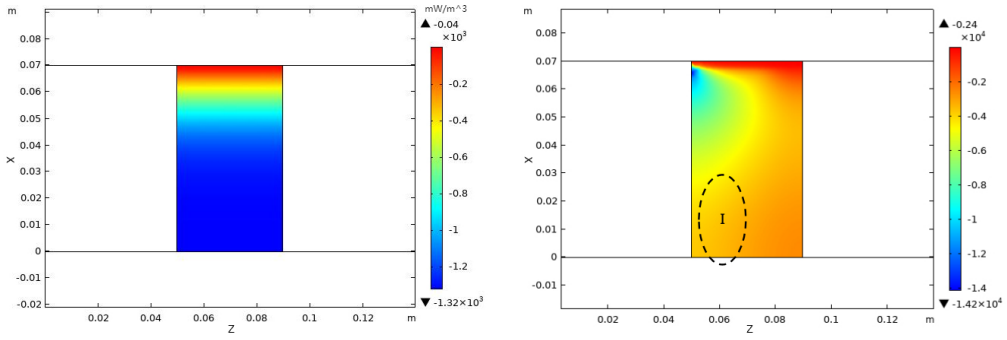

(a) The mode number is 2 (b) The mode number is 5

Fig. 7. Power deposition of TM waves of different mode number through the plasma

The power deposition of TM waves of different modes through the plasma is shown in Fig. 7. The power deposition due to the TM wave with mode number 2 in Fig. 7(a) is almost always at the irradiated end of the plasma. In contrast, the power deposition introduced by the TM wave with mode number 5 in Fig. 7(b) occurs mostly at the top surface of the plasma. The simulation results show that the mode number is one of the factors affecting the plasma power deposition.

3.2.2 Different Modes

In order to investigate the propagation of different modes of waves in plasma, the electron rate distribution, collisional power loss, and power deposition of TEM waves passing through the plasma are investigated in this section. Fig. 8 shows the electron rate distribution of the TEM wave generated by ionization of the plasma passing through the plasma at the same moment in Fig. 5.

The profile of this distribution is closer to that of Fig. 5(b), but the electron rate values are slightly different. The maximum value of the electron density is 2.16×10^{18} m^{-3}, and the minimum value is $4.92 \times 10^{13} m^{-3}$. Correspondingly, the contours of the collision loss power (Fig. 9(a)) and power deposition (Fig. 9 (b)) distributions are also similar to the results of the transmission of the TM wave with mode 5 (Figs. 6(b) and 7(b)). However, the corresponding amplitudes are all different. Therefore, there are also differences in the propagation modes of different Microwave Gaussian pulse light with respect to the plasma interaction.

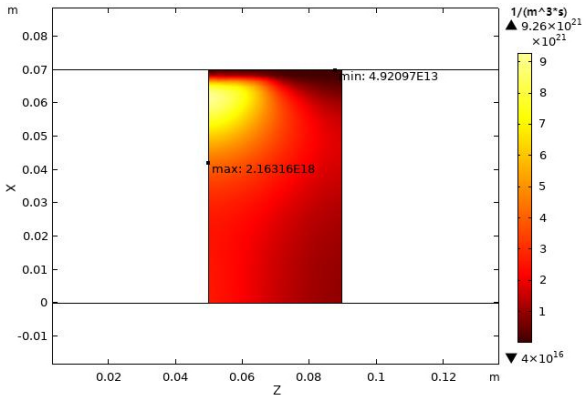

Fig. 8. Distribution of electron rates produced by ionization

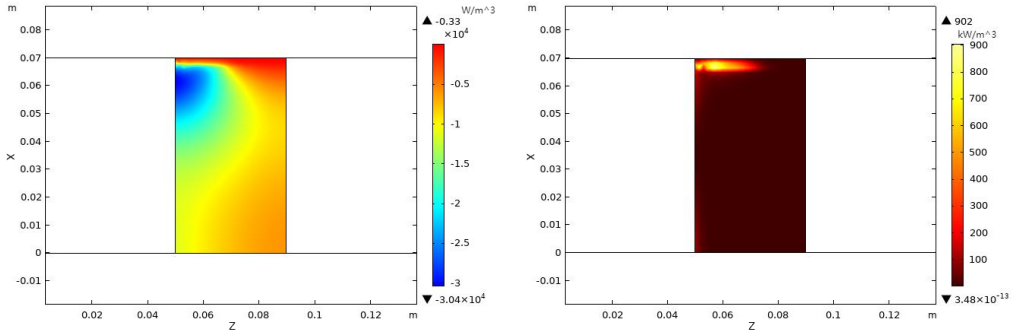

(a) Collisional power loss (b) Power deposition

Fig. 9. TEM wave propagation in plasma

3.3 Effect of Plasma Turbulence on Gaussian Pulsed Laser

The fluid instability and nonlinear effects present in plasma lead to irregular, chaotic and random flow states of fluid motion in plasma called plasma turbulence phenomena [22]. The anomalous effects caused by plasma turbulence result in transfer of transport energy and are an important research area in plasma physics and engineering. Fig.10(a) characterizes the electron rate distribution produced by ionization of the same Microwave Gaussian pulse light as in Fig. 2(a) after plasma turbulence. The maximum value of its electron density is $1.03 \times 10^{17} m^{-3}$, and the minimum value is $3.71 \times 10^{12} m^{-3}$. Comparison of Fig. 2(a) reveals that the presence of plasma turbulence increases the electron rate and electron density.

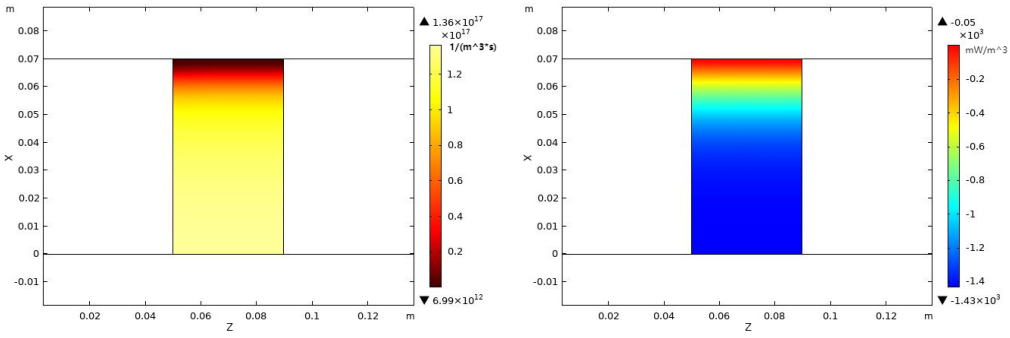

(a) (b)

Fig. 10. Microwave Gaussian pulse light through plasma turbulence: (a) electron rate profile； (b) collisional power loss

Fig. 10(b) shows the collisional power loss of Microwave Gaussian pulse light through plasma turbulence. It can be seen that the plasma turbulence does not change the direct correspondence between the electron rate distribution of the ionized plasma irradiated by Microwave Gaussian pulse light and the contour of the collision power loss distribution. However, compared to the collision power loss without considering the turbulence (Fig. 4(a)), the plasma turbulence has an effect on the electron rate and thus leads to a larger collision power loss.

Fig. 11 shows the power deposition distribution of Microwave Gaussian pulse light passing through the plasma and plasma turbulence, respectively. As can be seen in Fig. 11(a), the power deposition of Microwave Gaussian pulse light passing through the plasma is distributed at the irradiated end with a Gaussian profile. The power deposition passing through the plasma turbulence in Fig. 11(b) also occurs at the irradiated end of the plasma, but the presence of turbulence leads to a change in the distribution of its profile, and the presence of turbulence affects the distribution of the deposited power.

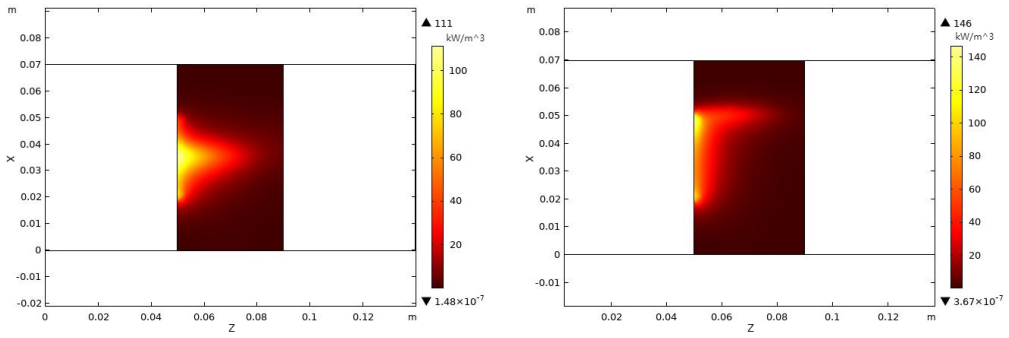

(a) Plasma (b) Plasma turbulence

Fig. 11. Power deposition distribution generated by Microwave Gaussian pulse light after (a) plasma (b) plasma turbulence

In summary, the presence of turbulence causes a transfer of the transmitted energy, leading to an increase in the power loss of the Microwave Gaussian pulse light passing through the plasma and affecting the transmission distribution of the light inside the plasma.

4. Conclusion

The objective of this study is to investigate the propagation characteristics of Microwave Gaussian pulse light with different frequencies, moduli, and modes in a plasma medium. In order to achieve this, numerical simulations are employed. The findings indicate that the rate distribution of electrons in a homogeneous plasma is not significantly affected by the use of Gaussian light with varying frequencies. Nevertheless, an increase in frequency affects the magnitude of the electron rate and the collision power loss resulting from plasma ionization by influencing the reaction energy and the distribution of the energy loss of high-frequency light in a plasma. This provides a reference for the selection of frequency for practical applications. Propagation of TM waves in plasma differs with mode number. The energy loss and transmission efficiency can be regulated by selecting the appropriate mode numbers. The impact of diverse wave modes on the electron rate, collisional power loss, and power deposition in the plasma is discernible, and these effects must be taken into account when selecting suitable wave modes to optimize transmission. The propagation of Microwave Gaussian pulse light in a turbulent plasma demonstrates that turbulence significantly increases the electron rate and electron density, as well as the power loss, which affects the power deposition distribution. This provides further insight into the mechanism of energy transport within the plasma.

The study presented in this paper provides a foundation for further research on the laser-plasma interaction and the propagation mechanism of Microwave Gaussian pulse light in plasma. This research is significant for the optimization of signal transmission and energy management of electromagnetic waves/lights in turbulent plasma. The subsequent step will be to study the propagation characteristics of Microwave Gaussian pulse light with a greater number of frequencies and modes in plasma with varying turbulent states.

Acknowledgment

This work was supported by the Yili Normal University Graduate Student Research and Innovation Project (No.YSD2025CX07);National Natural Science Foundation of China (Grant Nos. 12065023); Key Laboratory Project for Signal Detection and Control Technology (No.XHYB202302); the school-level Funding Project of Yili Normal University (No.2022YSQN001).

REFERENCES

[1] *E. Esarey, C.B. Schroeder, W.P. Leemans*, "Physics of laser-driven plasma-based electron accelerators", Review of Modern Physics, 81(3):1229-1285, doi:10.1103/RevModPhys.81.1229

[2] *V. Malka, J. Faure, C. Rechatin, A. Ben-Ismail, J. K. Lim, X. Davoine, E. Lefebvre,* "Laser-driven accelerators by collid ing pulses injection: A review of simulation and experimental results", Physics of Plasmas,16(5):495-501, doi:10.1063/1.3079486

[3] *K. Nakamura, A.J. Gonsalves, J.V. Tilborg, C.B. Schroeder, Cameron G. R. Geddes, E. Esarey*, "Laser Plasma Accelerator Experimental R&D at the BELLA Center", Journal of the Particle Accelerator Society of Japan,19(4):205-213, doi:10.50868/pasj.19.4_205

[4] *M. J. Keskinen, P. K. Chaturvedi, S. L. Ossakow,* "Long time scale evolution of high-power radio wave ionospheric heating 1. Beam propagation", Radio Science,28(5):775-784, doi: 10.1029/93RS00918

[5] *Olga P. Borchevkina, Sergey O. Adamson Adamson, Yurii A. Dyakov, Ivan V. Karpov, Gennady V. Golubkov, Pao-Kuan Wang, Maxim G. Golubkov*, "The influence of tropospheric processes on disturbances in the D and E ionospheric layers", Atmosphere, 2021, 12(9): 1116, doi: 10.3390/atmos12091116

[6] *Zhiqian Yin, Xin Zhou, Lin Lu, Chuanbo Zhang, Peng Xiang, Weiheng Dai, Yuliang Chen, Tao Fang, Zizhuo Li, Zhuoying Wang, Jiaqiang Nie, Xiangfei Chen*, "The influence of atmospheric turbulence-induced optical intensity scintillation on the accuracy of satellite-to-ground laser one-way timing", Advances in Space Research, 2024, doi: 10.1016/j.asr.2024.11.046

[7] *Xue Shen, Wei Kong, Tao Chen, Ye Liu, Genghua Huang, Rong Shu*, "An inter-satellite laser occultation method profiling atmospheric temperature and pressure from troposphere to lower mesosphere", Journal of Quantitative Spectroscopy and Radiative Transfer, 2024, 328: 109174, doi: 10.1016/j.jqsrt.2024.109174

[8] *J. Ongena, A. Messiaen, Y. O. Kazakov, R. Koch, R. Ragona, V. Bobkov, K. Crombé, F. Durodié, M. Goniche, A. Krivska,* "Recent advances in physics and technology of ion cyclotron resonance heating in view of future fusion reactors", Plasma Physics and Controlled Fusion, 59(5), 054002, doi: 10.1088/1361-6587/aa5a62

[9] *M. Hashemzadeh, S. M. Baki, M. Momeni, A. R. Niknam*, "Resonance absorption of intense short laser pulse in near critical inhomogeneous plasma", Waves in Random and Complex Media, 2019, 29(2): 215-226, doi: 10.1080/17455030.2018.1425571

[10] *Kazem Ardaneh, Remi Meyer, Mostafa Hassan, Remo Giust, Chen Xie, Benoit Morel, Ismail Ouadghiri-Idrissi, Luca Furfaro, Luc Froehly, Arnaud Couairon, Guy Bonnaud, Francois Courvoisier,* "High energy density plasma mediated by collisionless resonance absorption inside dielectrics", arXiv preprint arXiv:2109.00803, 2021 doi: 10.48550/arXiv.2109.00803

[11] *Srimanta Maity, Laxman Prasad Goswami, Ayushi Vashistha, Devshree Mandal, and Amita Das*,"Mode conversion and laser energy absorption by plasma under an inhomogeneous external magnetic field", Physical Review E, 2022, 105(5): 055209, doi: 10.1103/PhysRevE.105.055209

[12] *Xuan Gao, Yiping Han, Jiajia Wang*,"Propagation characteristics of the Bessel-Gaussian beams in turbu lent plasma sheath surrounding the hypersonic aerocraft",Journal of Quantitative Spectroscopy and Radiative Transfer, 2024, 322: 109017, doi: 10.1016/j.jqsrt.2024.109017

[13] *P. Monot, T. Auguste, P. Gibbon, F. Jakober, G. Mainfray, A. Dulieu, M. Louis-Jacquet, G. Malka, and J. L. Miquel*, "Experimental Demonstration of Relativ istic Self-channeling of a

Multiterawatt Laser Pulse in an Underdense Plasma", Phys. Rev. Lett.,74: 2953-2956, doi: 10.1103/PhysRevLett.74.2953

[14]*S.Y. Chen, G. S. Sarkisov, A. Maksimchuk, R. Wagner, D. Umstadter*. "Evolution of a Plasma Waveguide Created during Relativistic-ponderomotive Self-channeling of an Intense Laser Pulse", Phys. Rev. Lett., 1998, 80: 2610-2613, doi: 10.1103/PhysRevLett.80.2610

[15]*Z.H. He, B. Hou, V. Lebailly, J.A. Nees, K. Krushelnick, A.G.R. Thomas*, "Coherent control of plasma dynamics", Nature communications, 2015, 6(1): 7156, doi: 10.1038/ncomms8156

[16]*A. Köhn, E. Holzhauer, J. Leddy, M.B. Thomas*, R.G.L. Vann, "Influence of plasma turbulence on microwave propagation", Plasma Physics and Controlled Fusion,58(10), doi: 10.1088/0741-3335/58/10/105008

[17]*J.T. Li, S.F. Yang, L.X. Guo, M.J. Cheng, T. Gong*, "Power Spectrum of Refractive-Index Fluctuation in Hypersonic Plasma Turbulence", IEEE Transactions on Plasma Science, 45(9): 2431-2437, doi: 10.1109/tps.2017.2728865

[18]*A. K. Malik, K. P. Singh, B. P. Singh, S. Chaudhary, U. Verma*, "Terahertz Radiation Generation by Frequency Mixing of Hermite-Cosh-Gaussian Laser Beams in Density-Modulated Cold Magnetized Plasma", IEEE Transactions on Plasma Science, *49*(9), 3022-3028, doi: 10.1109/TPS.2021.3106960

[19]*A. Iantchenko*, "An experimental and computational study of tokamak plasma turbulence", EPFL, 2023

[20]*M.B. Mane, S.S. Patil, P.T. Takale, K.Y. Khandale, P.P. Nikam, P.P. Patil, M.V. Takale S.D. Patil*, "Propagation characters of dark and antidark Gaussian laser beams in collisionless magnetized plasma", Journal of Optics, 2024: 1-9, 10.1080/17455030.2022.2071500

[21]*Ning F.*Pulse Waveform Characteristics through Inhomogeneous Plasma with Modified WKB.Acta Electronica Sinica, 2010

[22]*M.H. Eghlidi, K. Mehrany, B. Rashidian*, "Modified WKB method for solution of wave propa gation in inhomogeneous structures with arbitrary permittivity and permeability profiles", 10.1109/EUMC.2007.4405459, doi: 10.1109/EUMC.2007.4405459

[23]*W. Chen, G. Zhu, Q. Deng, L. Yang, J. Li*, "Analysis of Gaussian beam broadening and scintillation in dex in anisotropic plasma turbulence", Waves in Random and Complex Media, 2022: 1-16, doi: 10.1080/17455030.2022.2071500